Robust H-infinity Control for DFIG to Enhance Transient Stability during Grid Faults

Sebastian Khoete, Yusuke Manabe, Muneaki Kurimoto, Toshihisa Funabashi and Takeyoshi Kato

***Abstract*—This paper proposes a new H-infinity robust control strategy for a grid-connected doubly fed induction generator based wind turbine (DFIG-WT) to improve transient stability during uncertainties and grid faults. A linearization scheme for the dynamic model of a DFIG is proposed, in which state space representation of DFIG has been derived in the stator-flux and grid-oriented reference frames. DC link voltage and rotor speed are selected and incorporated into the input disturbances in the input signals to enhance the stability of the H-infinity controller. Appropriate controllers are synthesized simultaneously for the rotor and grid side convertors of the DFIG subject to worst case disturbance. Extensive simulation studies are carried out on a 1.5 MW DFIG-WT connected to a power system consisting of a double-circuit transmission line. This is done to examine the operation and effectiveness of the proposed control method under disturbances and grid faults. As per simulation results, the proposed H-infinity controller provides improved and superior performance in terms of damped oscillations and less severe voltage dip in comparison with the commonly used PI controller.**

***Index Terms*— Doubly fed induction generator (DFIG), grid faults, H-infinity control, power system stability, wind power generation**

I. Introduction

DURING the last decades, the integration of renewable energy units such as wind power generation into the existing power system has been increasing, leading to high penetration of wind turbines (WT). The high penetration of WT in the power system, however, raises critical challenges with regard to the power quality in normal conditions and the grid stability during grid faults. Therefore, it has been recognized that WT controllers should play a critical role in the stability performance of grid-connected WT.

A doubly fed induction generator (DFIG) is a dominant type in wind power generation because of its advanced active/reactive power controllability. In order to fully utilize its controllability, DFIG controllers must be designed carefully and appropriately. However, the control of DFIGs has proven to be a difficult task because of several reasons including, nonlinear system dynamics, multivariable system, and unmeasurable state variables.

The vector control strategy is used for active and reactive power control of the DFIG-WT. Traditionally, the control function in the vector control is performed by PI control because it is simple and relatively easy to implement. However, because of the nonlinearity of the DFIG electrical dynamics, the conventional PI control methods are not ideal during uncertainties and grid faults. According to [1], there are two drawbacks associated with implementing PI current regulators in the DFIG design. Firstly, the discrete operation of the convertors is not taken into account. Secondly, the DFIG is modelled as a linear time-invariant system. Based on these simplifying assumptions, the gains of the PI controller are tuned using the small signal analysis of the nonlinear equations describing the DFIG behavior. Consequently, the system formulation is only valid around a specific operation condition, although the system is required to work properly at operating conditions largely deviated from nominal condition such as during grid faults.

The major concern in the design of advanced controllers for power systems is the ability of the control scheme to perform satisfactorily under a broad range of operating conditions that may involve uncertainties [3]. This is referred to as robustness capability. Robustness is particularly important in the DFIG control design in order to synthesize controllers that can maintain a high performance during grid disturbances and parameter uncertainties. There are some preceding studies based on the application of advanced control of the DFIG. For example, in [2], the authors developed a goal heuristic dynamic programming (GHrDP) based controller for the DFIG to improve transient stability during disturbances. Another study was done in [4], in which a nonlinear control method for a DFIG using differential geometry theory is proposed and compared with the traditional PI method. However, this method does not show significant improvement in the results. Reference [5] presents a sensitivity analysis approach based on both trajectory and frequency domain information integrated with evolutionary algorithm to achieve the optimal control of DFIG-WT, although this method does not take the nonlinearity of the DFIG into consideration during the controller design.

H-infinity control is one of the promising control schemes to overcome the above described drawbacks in the conventional control schemes. The robust H-infinity control has been studied extensively in the last three decades. Typical applications for robust control include systems that have high requirements for robustness to parameter variations and high requirements performances. The formulation of the H-infinity control problem is based on the minimization of a quadratic cost function that comprises both the disturbance and control input effects. One of the key features of H-infinity technique is the minimization of

Manuscript received July 03, 2016; revised August 04, 2016.

S. Khoete, Y. Manabe, M. Kurimoto, T. Funabashi, and T. Kato are with the Department of Electrical Engineering at Nagoya University, Nagoya, Japan (phone: +81 052 789 2036; fax: +81 052 789 2108; e-mail: s_koete@echo.nuee.nagoya-u.ac.jp).

ISBN: 978-988-14048-2-4
ISSN: 2078-0958 (Print); ISSN: 2078-0966 (Online)

noises and external disturbances without making assumptions on them.

However, there is barely any researches done to evaluate the performance of H-infinity control in the DFIG in order to improve transient stability during grid faults. A study based specially on the application of H-infinity control to wind power generation was done in [3], where a pitch control scheme and a model based H-infinity synthesis controller that yields a multivariable control law governing operation of the power electronic converter for a megawatt class DFIG over the entire operating trajectory is proposed. However, this study only focuses on pitch control of the WT during high wind turbulence. It does not investigate the behavior of the power system during grid and other disturbances. It also does not show comparison with other conventional methods.

In light of the above mentioned shortcomings, this study aims to propose a useful DFIG-WT control design strategy based on H-infinity control to improve transient stability during grid faults. Since robustness is an important issue in control systems design, special focus is placed on robustness of the system to external disturbances. To design the H-infinity controller, initially the system is represented in a standard configuration. Variables in the standard configuration, especially the exogenous input variables, are carefully selected and evaluated such that optimum controller performance is achieved.

The organization of this paper is as follows. Section II provides the mathematical modeling of the power system components under consideration and the theory of vector control. The proposed H-infinity control design algorithm and objectives are presented in Section III. In Section IV, the performance of the H-infinity, as well as PI controller, is demonstrated through a series of simulation results. Detailed interpretation of simulation results is also done in this section. Finally, concluding remarks are given in Section V.

II. System Configuration and Modeling

A. DFIG Model Configuration

Figure 1 illustrates the schematic of the wind turbine model studied in this paper. It represents a DFIG-WT consisting of a wound rotor induction type generator in which the stator windings are directly connected to the 60 Hz three-phase grid, and the rotor windings are fed through 3-phase back-to-back insulated-gate bipolar transistor (IGBT) based pulse width modulation (PWM) converters. The back-to-back PWM converter consists of a rotor-side converter (RSC), a grid-side converter (GSC) and a dc-link capacitor. Their controllers include three parts: a RSC controller, a GSC controller, and a wind turbine controller. The RSC and GSC controllers control the active and reactive power of the DFIG using the conventional vector control technique. Furthermore, the functions of these controllers are to produce smooth electrical power with constant voltage and frequency to the power grid whenever the wind system is working at sub-synchronous speed or super-synchronous speed, depending on the velocity of the wind [2].

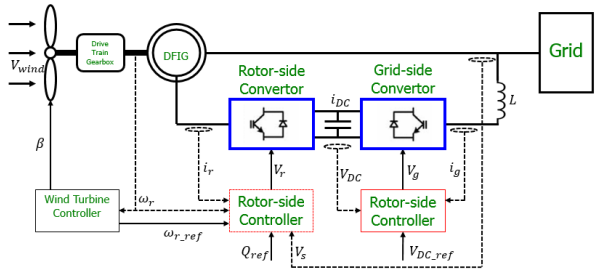

Figure 1. Schematic of a DFIG

The RSC aims to control the DFIG output active power and to maintain terminal voltage. In order to decouple the electromagnetic torque and the rotor excitation current, the induction generator is controlled in the stator-flux oriented reference frame, which is synchronously rotating, with its d-axis oriented along the stator-flux vector. Thus, the active power and voltage are controlled independently via *dq*-axis rotor voltage [2]. The voltage or the reactive power at grid terminals is controlled by the reactive current flowing in the converter. The GSC aims to maintain the DC-link voltage and to control the terminal voltage. In order to obtain independent control of the active and reactive power flowing between the grid and the grid side convertor, the convertor control operates in the grid voltage oriented reference frame, which is synchronously rotating, with its *d*-axis oriented along the grid voltage vector position. Thus, the DC-link voltage and reactive power are independently controlled via the *dq*-axis grid voltage [2]. In both the RSC and GSC, cross coupling between *dq*-axes components in the induction generator are considered as disturbances to enhance the stability of the system.

Figure 2 shows the field-oriented vector control system as implemented in this study. It was recognized that the proper determination of v^*_{dr} and v^*_{qr} in the PI current regulators plays an important role in the stability performance of the DFIG, because the PI regulators determine the control output which is used in the PWM converter. Thus, the proposed method replaces these synchronous-frame PI

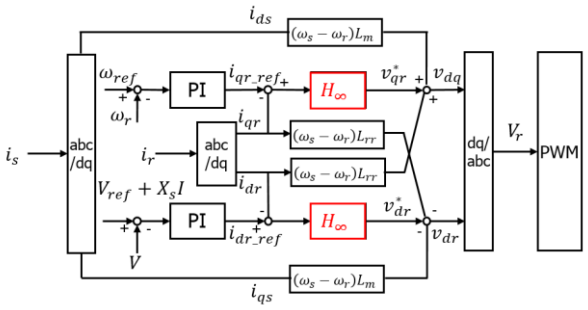

(a) Vector control implementation of H-infinity controller in RSC

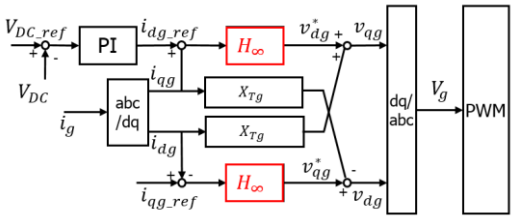

(b) Vector control implementation of H-infinity controller in GSC

Figure 2. Vector control implementation of H-infinity controller

ISBN: 978-988-14048-2-4
ISSN: 2078-0958 (Print); ISSN: 2078-0966 (Online)

current regulators with the robust H-infinity controllers as shown in Figure 2. Appropriate controllers are synthesized for the RSC and GSC. This is because the machine operation is fully controlled through the RSC, while GSC is mainly targeted to maintain DC link voltage because the RSC requires a constant voltage supply to operate. Therefore, the proposed H-infinity control strategy in this study aims to limit DC voltage fluctuations and to limit inrush rotor current during grid faults to protect the RSC and the rest of the power system.

In order to make a comparative analysis, the PI controllers designed in this study are of first order (K_P+K_I/s), which have the same input and output signals as the designed H-infinity controller. The PI controller parameters are tuned by trial-and-error approach.

B. DFIG Model Configuration

In this study, the space vector approach is adopted for the dynamic modelling of the electrical system, based on the fifth-order two-axis representation. The fifth-order dynamic equations describing the doubly fed induction generator are obtained by transforming the standard three-phase induction machine equations into a synchronously rotating reference frame in the direct and quadrature axes based on the current direction [3].

The respective three-phase stator and rotor voltages are obtained by the following DFIG electrical equations:

$$\begin{aligned} v_s &= R_s i_s + \frac{d}{dt}\psi_s - \omega_{ref}\psi_s \\ v_r &= R_r i_r + \frac{d}{dt}\psi_r - (\omega_{ref} - \omega_g)\psi_r \end{aligned} \tag{1}$$

where v_s and v_r are stator and rotor winding voltages; R_s, R_r, i_s and i_r are the stator and rotor winding resistances and currents; ω_{ref}, ω_n, ω_g are the reference, nominal and generator speeds, respectively, ψ_s and ψ_r are stator and rotor fluxes. The three phase quantities: voltages and fluxes can be determined as follows [3].

$$\begin{bmatrix} v_{ds} \\ v_{qs} \\ v_{dr} \\ v_{qr} \end{bmatrix} = [R^*]\begin{bmatrix} i_{ds} \\ i_{qs} \\ i_{dr} \\ i_{qr} \end{bmatrix} + \frac{d}{dt}\begin{bmatrix} \psi_{ds} \\ \psi_{qs} \\ \psi_{dr} \\ \psi_{qr} \end{bmatrix} + [\Omega^*]\begin{bmatrix} \psi_{ds} \\ \psi_{qs} \\ \psi_{dr} \\ \psi_{qr} \end{bmatrix} \tag{2}$$

$$R^* = \begin{bmatrix} R_s & 0 & 0 & 0 \\ 0 & R_s & 0 & 0 \\ 0 & 0 & R_r & 0 \\ 0 & 0 & 0 & R_r \end{bmatrix}, \quad \Omega^* = \begin{bmatrix} 0 & -\omega_0 & 0 & 0 \\ \omega_0 & 0 & 0 & 0 \\ 0 & 0 & 0 & -\Delta\omega \\ 0 & 0 & \Delta\omega & 0 \end{bmatrix}$$

where $\Delta\omega = (\omega_s - \omega_r)$; ω_s is the synchronous speed (rotational speed of the magnetic field); ω_r is the rotor rotational/electrical speed; R_s and R_r are stator and rotor winding resistances; subscripts *d* and *q* mean the *dq*-axis components. The flux linkages are expressed by the following sets of equations:

$$\begin{bmatrix} \psi_{ds} \\ \psi_{qs} \\ \psi_{dr} \\ \psi_{qr} \end{bmatrix} = \begin{bmatrix} L_s & 0 & L_m & 0 \\ 0 & L_s & 0 & L_m \\ L_m & 0 & L_r & 0 \\ 0 & L_m & 0 & L_r \end{bmatrix}\begin{bmatrix} i_{ds} \\ i_{qs} \\ i_{dr} \\ i_{qr} \end{bmatrix} \tag{3}$$

where L_s and L_r are stator and rotor winding inductances, and L_m is the mutual inductance.

A. DFIG Model Configuration

The drive train of the DFIG consists of a turbine, a low and high speed shaft, and a gearbox that connects to the generator. The system adopted in this study is a two-mass model and it is represented by [2]:

$$\begin{aligned} 2H_t\frac{d\omega}{dt} &= T_m - T_{sh} \\ \frac{d\theta_{tw}}{dt} &= \omega_t - \omega_r \\ 2H_g\frac{ds_r}{dt} &= -T_{em} - T_{sh} \\ T_{sh} &= K_{sh}\theta_{tw} - D_{sh}\frac{d\theta_{tw}}{dt} \end{aligned} \tag{4}$$

Where H_t the inertia constants of the turbine; H_g the inertia constants of the generator; ω_t the angle speed; ω_r the generator rotor angle speed; θ_{tw} the shaft twist angle; K_{sh} the shaft stiffness coefficient; D_{sh} the damping coefficient; T_{sh} the shaft torque; T_m the wind torque; T_{em} the electromagnetic torque.

III. H-INFINITY CONTROL DESIGN

A. H-infinity control principle

In this study, the proposed H-infinity controller achieves robustness in the DFIG by controlling the electrical power exchanged between the stator and the grid power. It does this by controlling the active and reactive power independently. It also aims to limit voltage fluctuations during and after a grid fault. By so doing, it gives improved tracking response and good robustness against the machine's parameter variations. One of the advantages of H-infinity is its ability to stabilize internal dynamics. The basic concept of H-infinity control is to allow for uncertainty in the design of the fixed controller, thus, producing a robust controller that is insensitive to parameter variations or disturbances [3]. The major drawback of the proposed method is that it comes at a cost of computational burden and could be hard to realize in practice.

B. DFIG Model Configuration

The proposed H-infinity control method makes use of a generator model that is locally linearized and is used to compute the control law. The known robustness features of the H-infinity control enable to compensate for the errors of the approximate linearization, as well as eliminate the effects of external disturbances. To perform the linearization, dynamic equations are first derived from electrical equations in (1). These dynamic equations are then written in state-space form using (9).

To design the H-infinity controller, initially the system is represented in a standard configuration as shown in Figure 3. The physical representation of this configuration can be easily understood by referring to the detailed electrical implementation showing the H-infinity control configuration in Figure 4. The vectors are defined as follows: *w* is the exogenous input that represents the driving signals

ISBN: 978-988-14048-2-4
ISSN: 2078-0958 (Print); ISSN: 2078-0966 (Online)

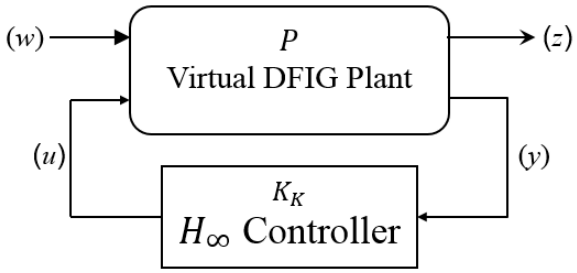

Figure 3. Standard H-infinity configuration

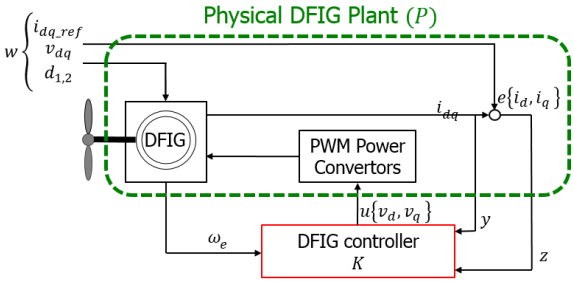

Figure 4. Detailed electrical implementation

generating the disturbances and input references signals; *u* is the control input vector which is responsible for closed loop stability; *z* denotes the error (output) signal we are trying to minimise, and ideally it should be zero; the observed output *y* is available for feedback; the vector *x* denotes the state variables.

In this study, variables in the standard configuration, especially the exogenous input variables, are carefully selected and evaluated such that optimum controller performance is achieved, that is, the H-infinity norm of the transfer function from inputs to outputs is minimum. H-infinity norm is used as a performance measure in this paper. The selected variables are as follows:

$$x = \begin{bmatrix} i_{ds} \\ i_{qs} \\ i_{dr} \\ i_{qr} \end{bmatrix}, \qquad w = \begin{bmatrix} i_{dr\_ref} \\ i_{qr\_ref} \\ v_{ds} \\ v_{qs} \\ d_1 \\ d_2 \end{bmatrix}, \qquad u = \begin{bmatrix} v_{dr} \\ v_{qr} \end{bmatrix} \tag{5}$$

$$y = \begin{bmatrix} i_{dr} \\ i_{qr} \end{bmatrix}, \qquad z = \begin{bmatrix} i_{dr\_ref} - i_{dr} \\ i_{qr\_ref} - i_{qr} \end{bmatrix} \tag{6}$$

$$d_1 = (\omega_s - \omega_r) L_m i_{qr}$$
$$d_2 = (\omega_s - \omega_r)(L_m i_{dr} + L_m \frac{V_{DC}}{R_r}) \tag{7}$$

The disturbance and reference terms are particularly considered because they incorporate electrical and physical dynamics of the system in the controller design. For instance, rotor speed is determined by the wind speed. As a result, the operating state of the wind turbine can be properly incorporated in the H-infinity controller design. This is unlike in conventional PI control methods where the parameters are fixed and not determined based on the operating state of the system. Furthermore, since the aim of the controller is to limit DC voltage fluctuations during a grid fault, it makes sense to incorporate DC link voltage in the disturbance formulation as seen in (7).

As mentioned earlier, the main difficulty of DFIG control during a grid fault is the system's nonlinear behavior. The linear controller does not perform satisfactorily in the case of grid faults or parameter variations. It is therefore essential that the nonlinearity of the system is considered in the controller design in order to synthesize a robust controller than can handle grid disturbances well. In order to achieve this objective, the plant model is carefully linearized from nonlinear variables to incorporate the inherent nonlinearity of the DFIG electrical dynamics in the controller design.

Finally, a stable and detectable state-space model for the continuous-time plant, *P*, is developed according to (8). The elements of (8) are matrices and are a result linearizing the DFIG dynamic model from the model equations in (1) and rewriting them until we get a reduced form shown in (9).

$$P: \begin{bmatrix} \dot{x} \\ z \\ y \end{bmatrix} = \begin{bmatrix} A & B_1 & B_2 \\ C_1 & D_{11} & D_{12} \\ C_2 & D_{21} & D_{22} \end{bmatrix} \begin{bmatrix} x \\ w \\ u \end{bmatrix} \tag{8}$$

$$\begin{aligned} \dot{x} &= Ax + B_1 w + B_2 u \\ z &= C_1 x + D_{11} w + D_{12} u \\ y &= C_2 x + D_{21} w + D_{22} u \end{aligned} \tag{9}$$

The H-infinity control problem is solved by searching for a controller *K* which internally stabilizes the closed-loop as in Figure 3. The control objective is then to minimize the H-infinity norm of the transfer function from inputs to outputs, such that it is less than a specified positive number, γ. That is:

$$\begin{aligned} \|T_{z\to w}\|_\infty &< \gamma, \qquad \gamma > 0 \\ T_{w\to z}(s) &= C_K(sI_n - A_K)^{-1}B_K + D_K \equiv K_K \end{aligned} \tag{10}$$

where *T* is the closed-loop transfer function from input *w* to output *z*.

Finally, the optimal H-infinity controller K_K is designed using state-space methods and using the information from (8). That is:

$$K_K(s): \begin{bmatrix} \dot{x}_K \\ u \end{bmatrix} = \begin{bmatrix} A_K & B_K \\ C_K & D_K \end{bmatrix} \begin{bmatrix} x_K \\ y \end{bmatrix} \tag{11}$$

The closed-loop data is obtained from (8) as:

$$\begin{aligned} A_K &= A + B_2 K C_2, & B_K &= B_1 + B_2 K D_{21} \\ C_K &= C_1 + D_{12} K C_2, & D_K &= D_{11} + D_{12} K D_{12} \end{aligned} \tag{12}$$

Numerical values for the aforementioned data are also determined analytically using the Robust Toolbox functions of MATLAB. The aim is to compute an output-feedback controller *K* that meets the design requirements such as internal stability and performance [6], [7].

In PI control, only two parameters, the proportional gain and integral gain, are required for the controller to operate. These parameters are also fixed and tuned around one operating point, meaning they do not depend on the operating state of the system. If case this operation point changes because of disturbances, the controller does not perform well since the parameters are fixed around one operating point. On the other hand, the H-infinity controller

ISBN: 978-988-14048-2-4
ISSN: 2078-0958 (Print); ISSN: 2078-0966 (Online)

in this study is designed to perform well regardless of the changing operating points. This is because the design incorporates the dynamics of the system in the controller design. The controller design makes use of a virtual plant model to estimate the controller parameters. This virtual plant is different from the physical plant of the DFIG which represents the process which is controlled by the control output. The virtual model can be visualized as in Figure 3 while Figure 4 can be thought of the physical process.

IV. Simulation Results

Figure 5 illustrates the diagram of the simulation model developed for this study. This power system model has been adopted and modified from MATLAB SimPowerSystems. A 9MW wind farm consisting of six 1.5 MW wind turbines with DFIG system connects to the utility grid via a 25kV 40km transmission line. The power is then exported through a 120kV grid through a feeder. The parameters of the DFIG and other power system components remain as given in the reference model in MATLAB.

After the proposed H-infinity controller is designed and developed, it is first tested in a simple benchmark network. When this step succeeds, the simulation model is modified in order to implement and test the developed controller in a more vulnerable and practical power system model as shown in Figure 5. This was done in order to verify the effectiveness and robustness of the proposed H-infinity controller under severe grid fault conditions. Major modifications include a double circuit transmission line; clearing the fault by means of a circuit breaker action; addition of synchronous generators to represent conventional generation; incorporation of dynamic and induction motor loads; and increasing the wind turbine capacity to simulate a mass wind penetration scenario.

During simulation, the wind speed is kept constant at 12m/s. A 3-phase fault of ground resistance 0.01 Ω is executed on the transmission line, 20km from B575 as seen in Figure 5. The fault is applied at 5 seconds and cleared after 0.15 seconds. Dynamics during a grid fault are recorded in Figure 6 and Figure 7. Simulations are performed with the purpose of evaluating the transient stability achievable with the proposed H-infinity controller and the conventional PI controller.

From Figures 6 and Figure 7 it can be seen that the PI controller results in oscillatory post-fault behavior. On the other hand, the H-infinity controller provides improved performance in terms of damped oscillations and a less severe voltage dip. Again from Figure 7 it can be seen that by using the H-infinity controller, the DC-link voltage fluctuation range is significantly reduced. This is important in order to protect the power convertors during severe grid fault conditions. In overall, the results illustrate superior performance of the H-infinity controller as compared to the PI controller.

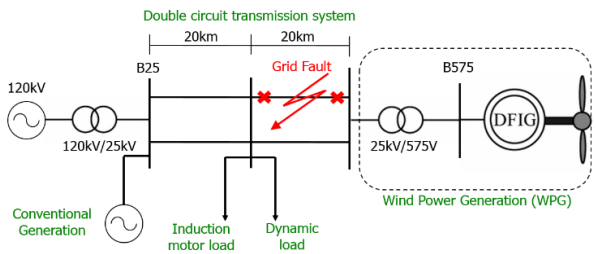

Figure 5. Vector control implementation of H-infinity controller

V. Conclusion

This paper presented a control design of a DFIG wind turbine based on H-infinity method in order to enhance transient stability during fault conditions. From the simulation results, it is apparent that the performance of the proposed H-infinity control approach is more effective than that of the conventional PI control. The fault ride through (FRT) of the DFIG wind turbine is significantly improved demonstrating the superiority of robust H-infinity control over conventional PI control. The future aim of this study is to investigate the effect of dynamic interactions of the controllers among several DFIG units. The importance of the proposed control method is that it can be used for future studies in robust control as well as modern wind turbine applications. It is suggested that the approach proposed in this paper could be practical for many control problems. It can also be extended to H-infinity design problems for decentralized control systems and descriptor systems.

References

[1] M. Mohseni , M. S. Islam and M. A. Masoum: “Enhanced hysteresis-based current regulators in vector control of DFIG wind turbine”, EEE Trans. Power Electron, Vol. 26, No. 1, pp. 223-234, 2011.

[2] Y. Tang, H. He, J. Wen and J. Liu, "Power system stability control for a wind farm based on adaptive dynamic programming," IEEE Transactions on Smart Grid, vol. 6, no. 1, pp. 166-177, 2015.

[3] B. Muhando and R. Wies, "Nonlinear H-infinity constrained feedback control for grid-interactive WECS under high stochasticity," IEEE Transactions on Energy Conversion. Vol. 26, No. 24, pp. 1000–1009, 2011.

[4] F. Wu, X. P. Zhang, P. Ju, and M. J. H. Sterling, "Decentralized Nonlinear Control of Wind Turbine with Doubly Fed Induction Generator," IEEE Transactions on Power Systems, Vol. 23, No. 2, pp. 613–621, 2008.

[5] Y. Tang; P. Ju; H. He; C. Qin; F. Wu, "Optimized Control of DFIG-Based Wind Generation Using Sensitivity Analysis and Particle Swarm Optimization," IEEE Transactions On Smart Grid, Vol. 4, No. 1, pp. 509–520, 2013.

[6] A. Abdul, N. Urasaki, A. Yona, T. Senjyu and A. Saber, "Design and Implement a Digital H-infinity Robust Controller for a MW-Class PMSG-Based Grid-Interactive Wind Energy Conversion System," Energies, Vol. 6, pp. 2084-2109, 2013.

[7] B. Muhando, T. Senjyu, A. Uehara, T. Funabashi, "Gain-Scheduled H∞ Control for WECS via LMI Techniques and Parametrically Dependent Feedback Part II: Controller Design and Implementation," IEEE Transactions on Industrial Electronics, Vol. 58, No. 1, pp. 57–65, 2011.

ISBN: 978-988-14048-2-4
ISSN: 2078-0958 (Print); ISSN: 2078-0966 (Online)

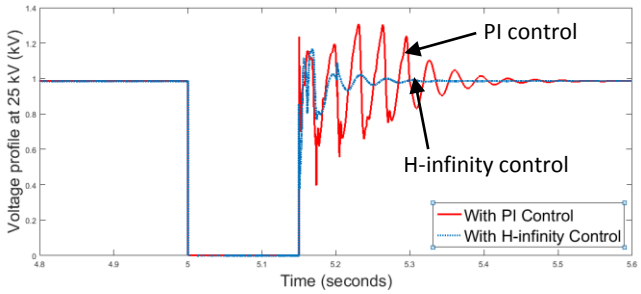

(a) Voltage profile (25kV transmission line)

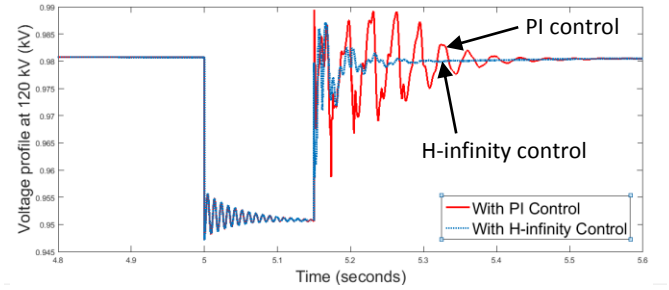

(b) Voltage profile (120kV transmission line)

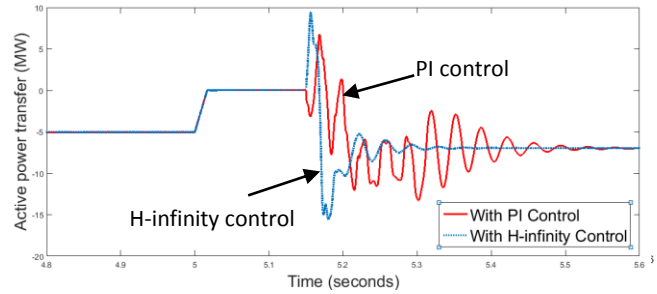

(c) Active power transfer

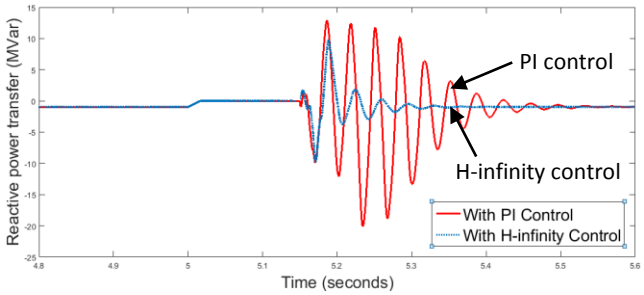

(d) Reactive power transfer

Figure 6. Comparison of system dynamics in the transmission system

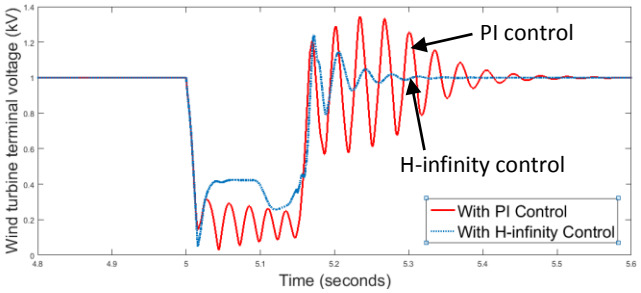

(a) Wind turbine terminal voltage

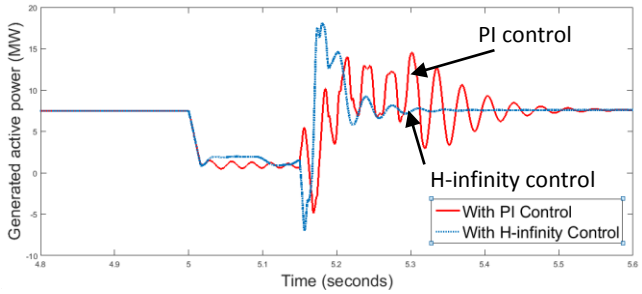

(b) Generated active power

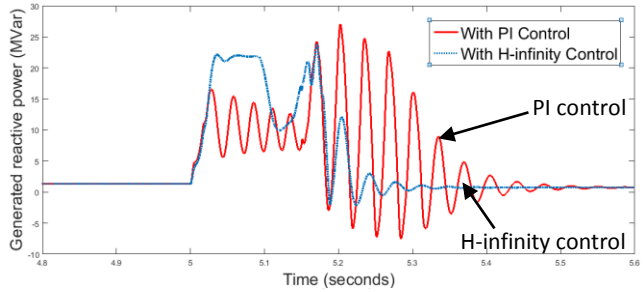

(c) Generated reactive power

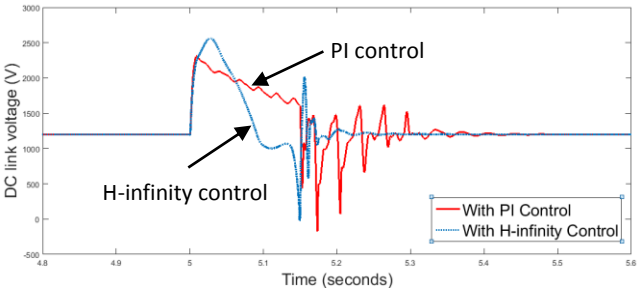

(d) DC link voltage

Figure 7. Comparison of system dynamics in the wind turbine

ISBN: 978-988-14048-2-4
ISSN: 2078-0958 (Print); ISSN: 2078-0966 (Online)